American Journal of Food Science and Technology, 2023, Vol. 11, No. 5, 183-188
Available online at http://pubs.sciepub.com/ajfst/11/5/3
Published by Science and Education Publishing
DOI:10.12691/ajfst-11-5-3

Numerical Study of Thermal Transfers in a Hohenheim-Type Mixed Solar Drying System Integrating Daily Solar Irradiation Data

Kokou Agbossou[1,*], Komi Apélété Amou[1], Tchamye T. E. Boroze[1], Kossi Napo[1], Andre D.L. Batako[2]

[1]Laboratoire sur l'Energie Solaire, Département de physique, Faculté des Sciences, Université de Lomé, BP : 1515 Lomé, Togo
[2]Genaral Engineering Research Institute, Liverpool John Moores University, Byrom Street, Liverpool, L3 3AF, UK
*Corresponding author: atheophile124@yahoo.fr

Received October 10, 2023; Revised November 14, 2023; Accepted November 21, 2023

Abstract This study focuses on a drying system consisting of a flat air solar collector coupled longitudinally to a drying chamber in the climatic conditions of tropical regions and the case of Togo was presented. The study was carried out using mathematical models obtained by writing the laws of energy conservation in the different components of the system. Simulations were achieved using experimental measurements of daily solar radiation and ambient temperature on a typical day in Lomé (Togo). The results highlight the importance of solar radiation and the use of fins on the performance of the drying system. It reveals that an optimal range of solar daily radiation for the proposed insulator for drying is 400 W/m^2 to 1000W/m^2, with an ambient air speed of 1.5 m/s to 4.5 m /s and a temperature variation of 20°C to 45°C.

Keywords: *solar drying, modeling, simulation, performance*

Cite This Article: Kokou Agbossou, Komi Apélété Amou, Tchamyè T. E. Boroze, Kossi Napo, And Andre D.L. Batako, "Numerical Study of Thermal Transfers in a Hohenheim -Type Mixed Solar Drying System Integrating Daily Solar Irradiation Data." *American Journal of Food Science and Technology*, vol. 11, no. 5 (2023): 183-188. doi: 10.12691/ajfst-11-5-3.

1. Introduction

Traditional drying, which is often done on the ground in the open air, is the most widely utilized method in developing nations since it is the simplest and cheapest form of food preservation [1-7]. Plants, seeds, vegetables, fruits, meat, fish, and other agricultural commodities have been preserved using traditional open-air solar drying methods for generations [2,6]. Because of the need for a vast area, the risk of quality degradation, air pollution, and bird and insect infestation, and intrinsic problems in managing the drying process, open-air drying has been increasingly limited during the last few decades [7,8]. Solar thermal technology is quickly gaining traction as an energy-saving strategy in agricultural applications where sunlight is abundant. Solar energy is favored above other alternative energy sources like the wind because it is abundant, inexhaustible, and nonpolluting [7]. Such data is also required for the most efficient design and study of solar energy conversion devices [1]. Alternative energy sources must be used to replace nonrenewable and polluting fossil fuels to meet the present rising energy demand and growing environmental concerns. Alternative energy sources include solar energy.

Solar dryers are easy to build with locally available tools and materials and can operate by natural convection. Drying requires energy and heat depending on the humidity content of the air, the drying system used, the drying temperature, the specifics of the product concerned (thickness, surface area, and air resistance), and the humidity contained in the element to be dried [9-14]. The performance of the dryer directly depends on the amount of irradiation and the humidity of the place of use. Finally, solar drying has become a practical solution with several advantages.

Currently, calculations for the construction of dryers are made on an empirical basis, especially given by the experience of the manufacturer. The objective of this work is the thermal study of a mixed solar dryer to characterize its effectiveness in drying agricultural products in climatic conditions in tropical regions. A simulation model is developed based on a thermodynamic approach to the elements and conditions involved in which the external climatic conditions (solar radiation, external temperature, relative air humidity) are variable over time.

Our dryers are made up of two parts: the solar collector and the drying cabin see Figure 1. Concerning the solar air collectors, the thermal efficiency can be improved if we promote the heat exchange between the absorption plate and the 'air. This model of the dryer is mainly dedicated to food production. It is intended mainly for tropical and subtropical regions and is in commercial operation in around sixty countries around the world. The Tunnel dryer uses photovoltaic cells to power the fans and thus circulate

the air in the drying area. The fan reduces drying time considerably. The air flows through an area usually painted black (collector area) to absorb heat from the sun and passes through the trays that hold the products intended to be dried.

A one-dimensional numerical model describing all the heat transfer modes involved was established. The unsteady thermal air entry conditions into the system were taken into account.

1. Air Inlet
2. Fan
3. Solar Module
4. Solar Collector
5. Side Metal Frame
6. Outlet of Collector

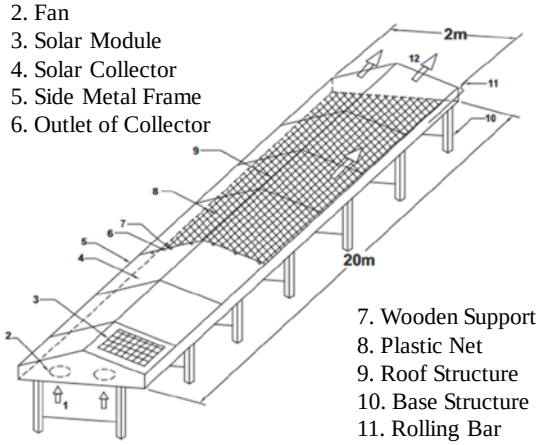

7. Wooden Support
8. Plastic Net
9. Roof Structure
10. Base Structure
11. Rolling Bar
12. Outlet of Drying tunnel

Figure 1. Hohenheim-Ttype solar tunnel dryer

2. Mathematical Modelling

We have formulated the following simplifying hypotheses:

- The reflection of radiative fluxes is neglected on the surface of the plastic film and the absorber
- The space between the insulator and the absorber is negligible
- One-dimensional heat and mass transfers
- The constant physical properties of materials and air
- the drying air is likened to an ideal gas
- $T_{amb} = T_{sol}$

Taking into account the simplifying hypotheses formulated above and the application of Ohm's law to the electrical network, we arrive at the following equations that govern the transfers in the sensors:

At the level of the plastic film cover

$$\frac{m_1 C_{P1}}{S_1}\frac{\partial T_v}{\partial t} = h_{r1}\left(T_c - T_v\right) + h_{r2}\left(T_{abs} - T_v\right) + h_{cv1}\left(T_{amb} - T_v\right) + h_{cv2}\left(T_{Fc} - T_v\right) \quad (1)$$

➢ Dry air temperature

$$m_2 C_{p2}\left(\frac{\partial T_{Fc}}{\partial t} + U.\frac{\partial T_{Fc}}{\partial x}\right) = h_{cv2} S_1\left(T_v - T_{Fc}\right) + h_{cv3} S_2\left(T_{abs} - T_{Fc}\right) \quad (2)$$

➢ absorber

$$m_3 C_{P3}\frac{\partial T_{abs}}{\partial t} = P_{abs} + h_{r3} S_3\left(T_v - T_{abs}\right) + h_{cv3} S_3\left(T_{Fc} - T_{abs}\right) + h_{cd} S_3\left(T_{iso} - T_{abs}\right) \quad (3)$$

➢ isolant

$$m_4 C_{P4}\frac{\partial T_{is}}{\partial t} = h_{cv4} S_4\left(T_{amb} - T_{iso}\right) + h_{cd} S_4\left(T_{abs} - T_{iso}\right) + h_{r4} S_4\left(T_{abs} - T_{iso}\right) \quad (4)$$

$$P_{abs} = \alpha_{abs} * \tau_v * S_2 * I \quad (5)$$

We obtained the following mathematical model:

$$\begin{cases} \frac{m_1 C_{P1}}{S_1}\frac{\partial T_v}{\partial t} = h_{r1}(T_c - T_v) + h_{r2}(T_{abs} - T_v) + h_{cv1}(T_{amb} - T_v) + h_{cv2}(T_{Fc} - T_v) \\ m_2 C_{p2}\left(\frac{\partial T_{Fc}}{\partial t} + U.\frac{\partial T_{Fc}}{\partial x}\right) = h_{cv2} S_1(T_v - T_{Fc}) + h_{cv3} S_2(T_{abs} - T_{Fc}) \\ m_3 C_{P3}\frac{\partial T_{abs}}{\partial t} = P_{abs} + h_{r3} S_3(T_v - T_{abs}) + h_{cv3} S_3(T_{Fc} - T_{abs}) + h_{cd} S_3(T_{iso} - T_{abs}) \\ m_4 C_{P4}\frac{\partial T_{is}}{\partial t} = h_{cv4} S_4(T_{amb} - T_{iso}) + h_{cd} S_4(T_{abs} - T_{iso}) + h_{r4} S_4(T_{abs} - T_{iso}) \end{cases} \quad (6)$$

It is a system of four equations with four unknowns, where T_v, T_{Fc}, T_{abs}, and T_{iso} represent the temperature of the plastic film, the air temperature, the absorber temperature, and the temperature of the insulating.

3. Thermal Balance in the Drying Unit

To simplify the study of coupled heat and mass transfers in which the dryer is the site, the following hypotheses are assumed to be valid:

To simplify the calculation, we do not take into account the heat exchanges within the product: We consider that the heat exchanges take place on the surface of the product;

- radiative exchanges inside the dryer are neglected;
- heat exchanges relating to the racks are neglected;
- the temperature and water content inside the product are assumed to be uniform;
- the products to be dried do not have a regular geometric shape;
- the products have the same temperature and have the same water content;
- The contact between the products and their support forms an adiabatic system.

Taking into account the previous hypotheses and considering that the drying area is divided into a certain number of fictitious slices, in the direction of the drying airflow, the equations that govern the thermal and mass exchanges at the level of the drying cabin translate into:

➢ Thermal assessment of the cover

$$\frac{m_1 C_{Pv}}{S_1}\frac{\partial T_{Fe}}{\partial t} = h_{r1}\left(T_{ciel} - T_v\right) + h_{r2}\left(T_{prod} - T_v\right) + h_{cv1}\left(T_{amb} - T_v\right) + h_{cv2}\left(T_{air} - T_v\right) \quad (7)$$

➢ Thermal balance of hot drying air

$$m_{air} C_{pair}\left(\frac{\partial T_{air}}{\partial t} + V.\frac{\partial T_{air}}{\partial x}\right) = h_{cv2} S_1\left(T_v - T_{air}\right) + h_{cv3} S_{prod}\left(T_{prod} - T_{air}\right) \quad (8)$$

➢ Thermal assessment of the product

$$m_{prod} C_{Pprod}\frac{\partial T_{prod}}{\partial t} = P_{prod} + h_{r3} S_{prod}\left(T_v - T_{prod}\right) + h_{cv3} S_{prod}\left(T_{air} - T_{prod}\right) - P_{ev} \quad (9)$$

$$P_{ev} = \dot{m}\left(T_{air}, H_{air}, D_{air}\right) * L_{ev}\left(T_{prod}\right) \quad (10)$$

$$L_{ev} = 4186,5\left(597 - 0,56 * T_{prod}\right) \quad (11)$$

A thermodynamic equilibrium is established.

➢ Water mass balance

The water mass losses or the quantity of water evaporated are expressed by the following equation:

$$\frac{dm}{dt} = m_{sec} * \left(-\frac{dX}{dt}\right) \quad (12)$$

Reminder of the concept of characteristic curve

The equation expressing the drying speed of the corn cobs will be deduced from the drying characteristic curve (C.C.S) translated in the form of a polynomial of degree three:

$$f\left(Xr\right) = \frac{\left(-\frac{dX}{dt}\right)}{\left(-\frac{dX}{dt}\right)_1} = X_{ro} + A * X_r + B * X_r^2 + C * X_r^3 \quad (13)$$

with $X_{ro} = 0,07077, A = -0,31299,$
$B = 0,45069 et C = -0,20432$

4. Resolution Method

The transfer equations obtained at the sensor and the drying cabin level are discretized using the implicit finite difference method based on their initial conditions and the associated limits. The algebraic system obtained was solved by the iterative method of Gauss-Seidel [9].

5. Results and Discussion

5.1. The Dry Air Temperature Profile in the Collector/Dryer

The temperature profile along the length of the dryer/collector for unloading conditions has been show in Figure (2). To show the variation of the temperature, three specifics hours in the day have been chosen. As seen in figure (2) the drying air temperature at 1:00 p.m. increases steadily, and the air temperature along the dryer was achieved to 70°C. The drying air temperature at 12:00 p.m. increases steadily, it ranges to 65°C. The drying air temperature at 9:00 a.m. increases steadily and that obtained around 60°C. The main observation is the significant difference between the temperature in the solar collector at different periods of the day for which the daily irradiation is very important. This difference is of the order of 6°C at 2:00 p.m. TSV [9,11]. At the unloading conditions, the drying air temperature increases steadily from the inlet of the collector up to the outlet of the drying chamber throughout the day. Similar result has found by Assefa and al. [18] using solar tunnel dyer for drying ginger.

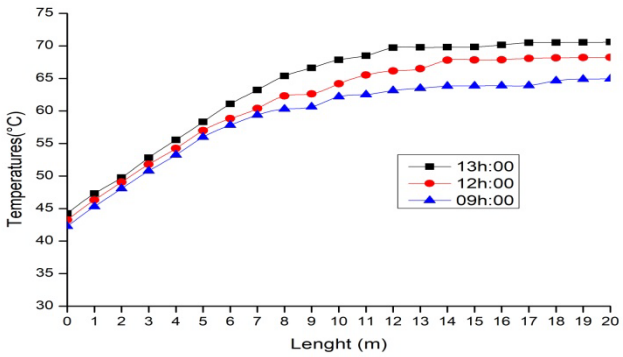

Figure 2. Temperature profile along the length of the dryer/collector

5.2. The Influence of the Insulator Area on Dry Air Temperature Profile in the Dryer

Figure (3) shows the influence areas of the insulator on the dry air temperature in the dryer. Five different areas of the insulator were made. They recorded that as soon as the surface of the insulator increase, the dry air temperature also increases. We notice on these graphs that the dry air temperature in this system solar dyer depended to the insulator surface. This could be related to the exchange surface between insulator and solar radiations influence the dry air temperature in the drying chamber, which is larger for the longitudinal convection.

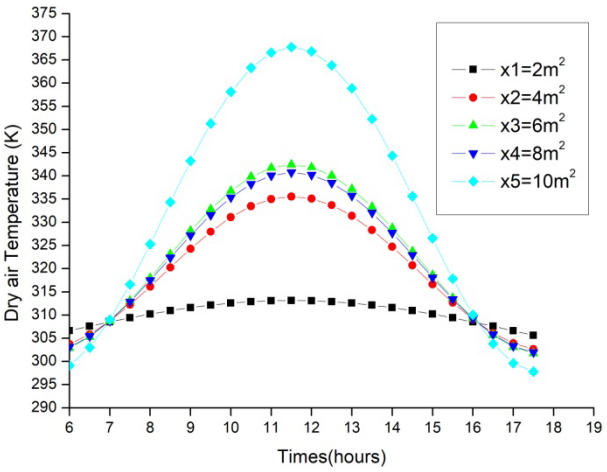

Figure 3. Evolution of the dry air temperature in the dyer as a function of time Vair =1.5m/s

5.3. Changes in Temperatures in the Drying Chamber

We have represented in Figure (4) the respective evolution of the air temperature, as a function of time for different levels. We observe a rise in temperature for the first sections between 6:00 a.m. TSV and 2:00 p.m. TSV. This can be explained by the fact that due to the increase in the density of the incident solar flux in the morning, the air temperature at the collector outlet is constantly increasing. For the other sections, this rise in temperature

occurs more slowly as we move away from the collector inlet. The mathematical model thus reflects the effect of the thermal inertia of the storage volume [4,5,6]. On the other hand, in the afternoon, the gradual decrease in the temperature of the air leaving the sensor causes a cooling of the collector inlet zone and the fluid passes through the collector from the hottest part towards the lowest part. The warmer zone gradually gives up all its stored energy to the colder zone. We then obtain at the outlet of the collector, a fluid temperature that gradually increases over time to reach a maximum around 6:00 p.m. TSV and then decreases again.

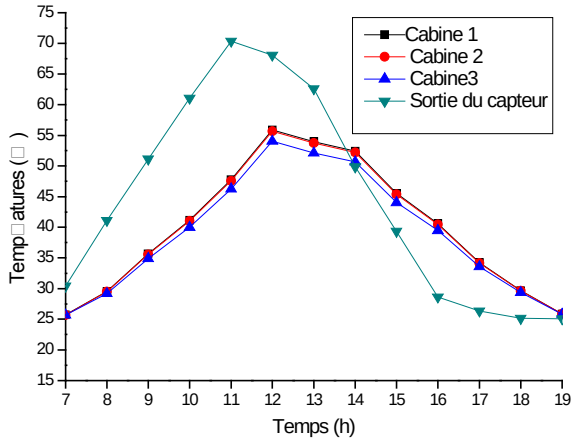

Figure 4. Evolution of the air temperature in the drying cabin at different levels as a function of time Vair =1.5m/s

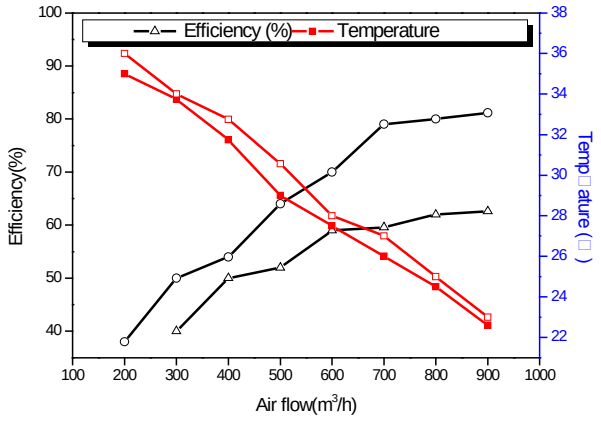

Figure 5. Variation de ΔT et du rendement en fonction de la densité

5.4. Influence of the Physical and Optical Properties of the Plastic Film Cover

Figure 4 shows that the profile of temperature and efficiency as a function of air density is compared for an insulator covered with polyethylene plastic film and an insulator covered with polymethacrylate film. We observe that, under the same conditions, the thermal performance of the polyethylene insulator is better compared to that of Polymethacrylate, with a maximum efficiency of 79.89%. This result is due to the physical properties of the plastic film which reduces the wavelength of ultraviolet solar radiation into a smaller infrared wavelength that can no longer be reflected by it.

Glass is the most effective material from this point of view. It absorbs 82% of infrared and only reflects 18%, transmitting almost none. Plastics have very diverse behaviors: 0.15mm thick polyethylene lets 73% of infrared rays pass through, while 0.10mm acetate only lets 20% pass through. Other plastic films fall between these two extremes.

5.5. Influence of Solar Fluxes

The optimization of a solar air insulator for drying agricultural products is not easy, because a multitude of factors come into play depending on different basic parameters such as the overall solar deposit on the horizontal plane, the temperature of the drying fluid (sensor output-cabin input), the wind speed in the area and the length of the insulator, etc. Figure 6 (a-f) presents the optimization criteria according to the combination of ambient temperature, solar flux, and drying air speed for an efficiency greater than 59.75%, which combines these different settings.

The first parameter that interests us is the solar flux which is difficult to control and which must be high (greater than 1000W/m^2). The objective set being to choose one of the couples that minimizes these quantities, we are led to opt for a maximum efficiency of the order greater than 60%.

The results show that a better efficiency of such a type of sensor for drying is between 400 W/m^2 to 1000W/m^2, an ambient air speed of between 1.5 m/s to 4.5 m /s, and an ambient temperature varying between 20°C and 45°C. To choose these parameters and the corresponding values, we exploited the graphs of yields versus speed for different climatic conditions and the effects of sensitivity. These results are in good agreement with those reported by Kiranoudis et al., Zomorodian, A., et al. Intawee, P. [19,20,21].

6. Conclusion

This study focused on the digital simulation of the performance of a mixed solar drying system operating in direct mode, coupled with an air circulation sensor painted black. Such characterization is very interesting because it allows a good understanding of the mechanisms taking place in the units studied for the dimensioning of the dryer used. We thus carried out a detailed modeling of the heat transfers in the main components of the solar collector and the drying unit. This study showed that the use of a black-painted absorber in the collector thus making it possible to increase the temperature of the hot air circulation remains an effective means for improving the performance of a solar collector coupled with a drying unit. The triplets of wind speed, drying hot air speed, and solar flux are very important in the solar drying system in tropical areas.

The results highlight the importance of solar radiation and the use of fins on the performance of the drying system. It reveals that an optimal range of solar daily radiation for the proposed insulator for drying is 400 W/m^2 to 1000W/m^2, with an ambient air speed of 1.5 m/s to 4.5 m /s and a temperature variation of 20°C to 45°C.

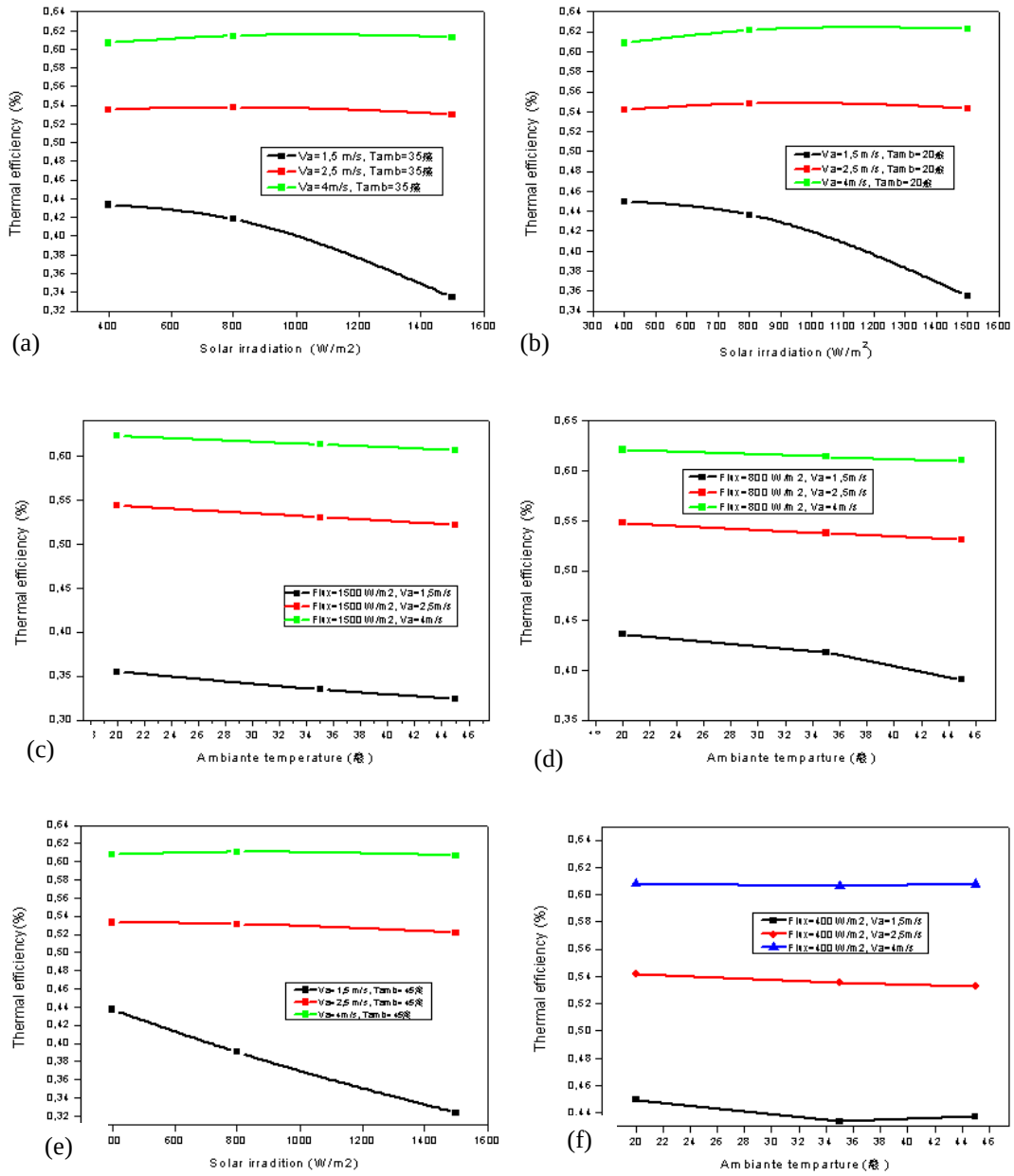

Figure 6. Optimization criteria according to the combination of ambient temperature, solar flux, and drying air speed

ACKNOWLEDGMENTS

The author would like to acknowledge all the members of "LAboratoir de Mathématique Et de PhySique – Groupe de Mecanique Energetique (LA.M.P.S.-G.M. E)" in France for the workshop facility and technical support throughout this research work.

Nomenclature

S *Exchange surface (m^2)*
S_1 *Surface area of solar collector (m^2)*
S_2 *Area of drying cabin (m^2)*
A *Surface area of the solar panel (m^2)*
C_p *Specific heat of the fluid (J/Kg. K)*
L_v *Latent heat of vaporization (J /Kg)*
Hr_1 *Radiation coefficient between the cover and the celestial vault (W/m^2. K)*
Hr_2 *Radiation coefficient between the cover and the absorber (W/m^2. K)*
Hr_3 *Radiation coefficient between the absorber and the cover (W/m^2. K)*
Hcv_1 *Coefficient of heat transfer by convection between the cover and the ambient environment (W/m^2. K)*
Hcv_2 *Coefficient of heat transfer by convection between the blanket and the heat transfer fluid (W/m^2. K)*
Hcv_3 *Coefficient of heat transfer by convection between the absorber and the heat transfer fluid (W/m^2. K)*
Hcv_4 *Coefficient of heat transfer by convection between the insulation and the ambient environment (W/m^2. K).*
H_{cd} *Coefficient of heat transfer by conduction between the absorber and the insulator (W/m^2. K)*
P_u *Power of the heat transfer fluid (W/m^2)*
P *Power per unit area (W/m^2)*

H_a *Absolute air humidity (Kg/kg)*
U *Overall loss coefficient*
D *Diffusion coefficient (m^2/s)*
m *Mass (Kg)*
D_m *Air mass flow (Kg/s)*
Dh *Water diameter (m)*
E *Insulation thickness (m)*
F *Cover form factor*
L *Cabin length (m)*
Lc *Sensor length*
H *Sensor height*
Gr *Grashof number*
Nu *Nusselt number*
R_e *Reynolds number*
P_r *Prandtl number*
Pa *Pressure (Pa)*
PV *Photovoltaic*
Q *Radiated solar flux density ($W.m^{-2}$)*
Q_0 *Solar flux density ($W.m^{-2}$)*
A *Product surface (m)*
DV *Air volume flow (m3/s)*
t *Time (s)*
T *Temperature (°C or K)*
T_C *Temperature of the celestial vault (°C or K)*
V_W *Wind Speed*
Vf *Speed of the heat transfer fluid (ms-1)*
X_R *Reduced water content*
X_t *Instantaneous water content*
Xi *Initial water content*
X_{cr} *Critical water content*
X_{eq} *Equilibrium water content*

Greek Letters

α *Absorptivity coefficient*
β *Thermal expansion coefficient*
Φ *Thermal flow (Energies J)*
τ_i *Inflation rate*
Ψ *Dimensionless current function*
Θ *Dimensionless temperature*
T *Transmission coefficient (radiation)*
E *Emissivity coefficient*
σ *Stefan-Boltzmann constant ($5{,}67.10^{-8} W.m^{-2}. K^{-4}$)*
μ *Dynamic viscosity of air (kg $m^{-1}s^{-1}$)*
ν *Kinematic viscosity of air (m^2s^{-1})*
ρ *Air density (kg^{-3})*
λ *Thermal conductivity coefficient ($Wm^{-1}°C^{-1}$)*
ηt *Instantaneous thermal efficiency*
η *Average thermal efficiency*

Clues:

iso *Thermal insulation*
op *optical*
v *Cover (plastic film)*
f *Heat transfer fluid*
Amb *Ambient*
c *sky*
cab *Cabin*
p *product*
w *wind*
e *Entrance*
s *Output dry*

References

[1] A. Bedri, Solar Thermal Energy Use as a Substitute for Residential Building in Ethiopia, California state University, Sacramento, 2013.

[2] S. A. Mekonen, Solar Energy Assessment in Ethiopia: Modeling and Measurement, Addis Ababa University, 2007.

[3] A. Goetzberger and V. U. Hoffmann, Photovoltaic Solar Energy Generation, vol. 112, Springer Science & Business Media, 2005.

[4] G. D. RAI, Solar Energy Utilisation, Kanna Publishers, Delhi, 4th edition ed. edition, 2000.

[5] A. J. Mobolade, N. Bunindro, D. Sahoo, and Y. Rajashekar, "Traditional methods of food grains preservation and storage in Nigeria and India," Annals of Agricultural Sciences, vol. 64, no. 2, pp. 196–205, 2019.

[6] C. Loha, R. Das, and B. Choudhury, "Evaluation of air drying characteristics of sliced ginger (Zingiber officinale) in a forced convective cabinet dryer and thermal conductivity measurement," Journal of Food Processing and Technology, vol. 03, no. 06, 2012

[7] A. A. C. A. Ogunlade, "Physical properties of ginger (Zingiber officinale)," Global Journal of Science Frontier Research, vol. 14, no. 8, 2014.

[8] A. A. Gatea, "Performance evaluation of a mixed-mode solar dryer for evaporating moisture in beans," Journal of Agricultural Biotechnology and Sustainable Development, vol. 3,no. 4, pp. 65–71, 2011.

[9] S. Oudjedi "Theoretical and experimental study of a solar air collector intended for drying", Renewable Energy Research Unit in the Saharan environment, Adar, Algeria 2008

[10] McAdams W.H. " Heat transmission",3rd ed. Mc. Graw Hill, New York, 1954.

[11] F. Mokhtar, «Etude théorique et expérimentale d'un capteur solaire à air destiné au séchage», Unité de Recherche en Energie Renouvelable en milieu Saharien, B.P478, Route de Reggane, Adar, Algérie 2008.

[12] S. Youcef-Ali» Etude numérique et expérimentale des séchoirs solaires indirects à convection forcée : Application à la pomme de terre», Thèse de Doctorat, Université de Valenciennes et du Hainaut-Cambrésis, France, 2001.

[13] Swinbank WC "Long–Wave radiation from clear skies". QJ Roy Meteor Soc 89, 1963.

[14] M. Daguenet, «Les Séchoirs Solaires, Théories et pratique», Unesco, 1985.

[15] T. Letz, «Modélisation et dimensionnement économique d'un système de chauffage domestique bi-énergie», Thèse de Doctorat INSA Lyon, 1985.

[16] Aissani Larbi «Study and construction of a solar dryer for fruits and vegetables» Master's dissertation, University of Constantine, 1988

[17] Assefa T." Fabrication and Performance Evalution of Solar Tunnel Dryer for Ginger Drying" International Journal of Photoenergy

[18] Assefa tesfaye & al. Fabrication and Performance Evaluation of Solar Tunnel dryer for Ginger Drying, International Journal of Photoenergy,pg.13, 2022

[19] C. T. Kiranoudis, Z. B. Maroullis, E. Tsami and D. Marinos-Kouris, "Equilibrium Moisture Content and Heat of Desorption of Some Vegetables," Journal of Food Engineering, Vol. 20, No. 1, 1993, pp. 55-74.

[20] Zomorodian, A., et al. (2007). Optimization and evaluation of a semicontinuous solar dryer for cereals (rice, etc.). Desalination, 209, 129–135.

[21] Intawee, P., & Janjai, S. (2011). Performance evaluation of a largescale polyethylene covered greenhouse solar dryer. International Energy Journal, 12, 39–52.